Synthesis, X-ray structures and NIR chiroptical properties of a series of dinuclear lanthanide(III) complexes [Ln₂{µ-(S- or RS-pba)}₄(HBpz₃)₂]; novel configurational chirality due to non-bonding Ln···O interactions †

Md. Abdus Subhan, Takayoshi Suzuki, Akira Fuyuhiro and Sumio Kaizaki*

Department of Chemistry, Graduate School of Science, Osaka University, Toyonaka, Osaka, 560-0043, Japan

Two series of mononuclear [Ln^{III}(S- or RS-pba)(HBpz₃)₂] (Ln = Tm, Er, Ho) and dinuclear [Ln₂{µ-(S- or RS-pba)}₄-(HBpz₃⁻)₂] (Ln = Yb, Ho, Gd, Dy, Nd) complexes (pba = RS- and/or S-2-phenyl butyrate, HBpz₃ = hydrotris(pyrazol-1-yl)borate) were prepared and their X-ray structures and NIR chiroptical properties investigated. Synthesis with a molar ratio 1 : 2 : 1 of Ln : KHBpz₃ : pba results in the formation of either mono- or dinuclear complexes, depending on the Ln(III) ionic radii: mononuclear complexes from Yb(III) to Ho(III) and dinuclear ones from Dy(III) to Nd(III). Only the dinuclear complexes for all of the Ln(III) studied were formed with a molar ratio 1 : 1 : 2 of Ln : KHBpz₃ : pba. X-Ray structural analysis confirmed dinuclear structures with CH ··· π interactions and linear B ··· Ln ··· Ln ··· B arrangements for the Ln(µ-RS-pba)₄Ln(HBpz₃)₂ (Yb, Ho, Dy, Gd and Nd) complexes and a skew bent arrangement of B ··· Ln ··· Ln ··· B leading to configurational chirality in the Dy(µ-S-pba)₄Dy(HBpz₃)₂ complex. Comparison of NIR chiroptical spectra in the 4f–4f transitions with those of the corresponding Cr–Ln complexes, [(acac)₂Cr(ox)Ln(HBpz₃)₂] suggests that the 4f–4f CD intensities arise from configurational chirality, probably due to the skew bent B ··· Ln ··· Ln ··· B disposition.

Introduction

Recently, there have been several investigations on configurational chiral Ln(III) complexes from respective points of view.[1] In the last few years we have been studying chiroptical spectra in the 4f–4f transitions of 3d–4f dinuclear complexes.[2–5] In this context, our recent paper[3a] was concerned with NIR CD spectra of the 4f–4f transitions of the configurational chiral 3d–4f (Λ–Δ)-[(acac)₂Cr(ox)Ln(HBpz₃)₂] (Ln = Dy and Yb) complexes with no asymmetric carbon. This followed the NIR CD study along most of the series of the 3d–4f Cr–Ln[3b] and the Co–Ln complexes[4] as well as a more recent study on variable temperature emission spectra,[5] which are devoted to the evaluation of the structural and NIR spectroscopic properties of the Cr(ox)Ln or Co(ox)Ln complexes. In our first paper,[3a] configurational chirality around the Yb(III) ion in the Cr(ox)Yb complex induced by optically resolved complex ligand Λ-[Cr(acac)₂(ox)]⁻ was examined in comparison to vicinal chirality in Λ,Δ-[Yb(S-pba)(HBpz₃)₂] (pba = RS- and/or S-2-phenyl butyrate, HBpz₃ = hydrotris(pyrazol-1-yl)borate). We attempted to prepare a whole series of mononuclear [Ln(S- or RS-pba)(HBpz₃)₂] complexes to compare with Cr(ox)Ln. The complexes [Ln(S- or RS-pba)(HBpz₃)₂] could be isolated for the heavier lanthanide(III) ions from Yb(III) to Ho(III). However, for the lighter Ln^{III} ions from Nd to Dy, preparation of [Ln(S- or RS-pba)(HBpz₃)₂] was unsuccessful, and complexes [Ln(S- or RS-pba)₂(HBpz₃)] were isolated with an apparently seven-coordinate structure. This chemical composition of the latter complexes is identical with that of the known tetracarboxylate bridged dinuclear Y(III) complex,[6] which takes a dinuclear structure analogous to that of the tetracarboxylate bridged Ce(III)[7] or Eu(III) and Nd(III) dimers.[8] This prompted us to perform X-ray analysis on [Ln(S-pba)₂(HBpz₃)], for which the near infrared photochemical properties have been preliminarily

reported.[5b] Over the last 15 years, dinuclear Ln–Ln complexes with bridging carboxylate type ligands have been studied from different view points.[6–10] The latest study on the benzoate bridged Ln(III) complexes focused on the synthesis, X-ray structures and emission properties, but the targeted lanthanide ions were limited to only three Gd and Tb complexes.[10] Though the metal–metal interactions and chiroptical properties for the tetracarboxylate bridged dinuclear transition metal complexes of the type, M₂(O₂CR)₄L₂ have been studied (showing only vicinal chirality due to optically active RCO₂) for a few decades,[11] there are no systematic chiroptical studies on this type of Ln₂(O₂CR)₄L₂ complexes with configurational chirality.

We report here the synthesis of the mononuclear [Ln(S- or RS-pba)(HBpz₃)₂] (Ln = Yb,[3] Tm, Er and Ho) and dinuclear [Ln₂{µ-(S- or RS-pba)}₄(HBpz₃)₂] (Ln = Yb, Ho, Dy, Sm and Nd) complexes with a change from mononuclear to dinuclear formation at Dy, depending on the ionic radius of the lanthanide(III) ion and/or by controlling the ratio of Ln : pba : KHBpz₃. The NIR CD of the chiral [Ln₂(µ-S-pba)₄(HBpz₃)₂] complexes along with the absorption and MCD of their racemic RS-pba analogues were studied in relation with the X-ray structures of the (Yb–Yb, Ho–Ho, Dy–Dy, Nd–Nd) complexes.

Experimental

Synthesis of mononuclear and dinuclear carboxylato complexes

The mononuclear [Ln(S- or RS-pba)(HBpz₃)₂] (Ln = Ho, Er, Tm, Yb) complexes were prepared with a molar ratio of 1 : 2 : 1 (Ln : HBpz₃ : pba) using a previously described method (Method A).[3a] The same Method A gave dinuclear complexes [Ln₂{µ-(S- or RS-pba)}₄(HBpz₃)₂] from Dy to Nd instead of the mononuclear ones. For this preparation, two products, one of which is soluble and the other insoluble in CH₂Cl₂, were obtained. The soluble one was found to be the dinuclear complex [Ln₂{µ-(S- or RS-pba)}₄(HBpz₃)₂], but the insoluble one was [Ln(HBpz₃)₃].

The dinuclear complexes [Ln₂{µ-(S- or RS-pba)}₄(HBpz₃)₂] (Yb, Ho, Dy, Gd and Nd) were prepared by Method B where

Table 1 Crystallographic data for Yb(μ-*RS*-pba)$_4$Yb(HBpz$_3$)$_2$ (**1**), Ho(μ-*RS*-pba)$_4$Ho(HBpz$_3$)$_2$ (**2**), Gd(μ-*RS*-pba)$_4$Gd(HBpz$_3$)$_2$ (**3**), Nd(μ-*RS*-pba)$_4$-Nd(HBpz$_3$)$_2$ (**4**), Dy(μ-*RS*-pba)$_4$Dy(HBpz$_3$)$_2$ (**5**) and Dy(μ-*S*-pba)$_4$Dy(HBpz$_3$)$_2$ (**6**)

	1	**2**	**3**	**4**	**5**	**6**
Formula	C$_{58}$H$_{64}$B$_2$N$_{12}$O$_8$-Yb$_2$	C$_{58}$H$_{64}$B$_2$N$_{12}$O$_8$-Ho$_2$	C$_{58}$H$_{64}$B$_2$N$_{12}$O$_8$-Gd$_2$	C$_{58}$H$_{64}$B$_2$N$_{12}$O$_8$-Nd$_2$	C$_{58}$H$_{64}$B$_2$N$_{12}$O$_8$-Dy$_2$	C$_{58}$H$_{64}$B$_2$N$_{12}$O$_8$-Dy$_2$
M	1424.91	1408.69	1393.34	1367.32	1403.83	1403.83
T/°C	23	23	23	23	23	-73
λ(Mo-K$_\alpha$)/Å	0.71069	0.71069	0.71069	0.71069	0.71069	0.71069
Crystal system	Triclinic	Triclinic	Triclinic	Triclinic	Triclinic	Monoclinic
Space group	$P\bar{1}$	$P\bar{1}$	$P\bar{1}$	$P\bar{1}$	$P\bar{1}$	$P2_1$
a/Å	11.551(2)	11.587(3)	11.610(3)	11.661(2)	11.589(5)	13.0708(13)
b/Å	12.222(3)	12.207(4)	12.185(3)	12.258(2)	12.174(5)	24.8098(18)
c/Å	12.6247(17)	12.622(3)	12.622(3)	12.637(2)	12.633(4)	19.2494(18)
α/°	80.159(16)	80.31(3)	80.72(2)	80.239(14)	80.52(3)	90
β/°	68.300(12)	68.43(2)	68.804(17)	68.926(13)	68.49(3)	103.903(4)
γ/°	66.306(16)	66.11(2)	65.780(19)	65.244(13)	66.12(3)	90
V/Å^3	1515.9(5)	1517.7(7)	1518.1(6)	1530.3(5)	1515.9(110)	6059.4(9)
Z	1	1	1	1	1	4
ρcalc./Mg m^{-3}	1.561	1.541	1.524	1.484	1.538	1.539
μ(Mo-K$_\alpha$)/mm^{-1}	3.128	2.650	2.228	1.739	2.508	2.510
$R1(F^2: F^2 > 2\sigma(F^2))$	0.038	0.049	0.047	0.050	0.065	0.093
$wR2(F^2:$ all data)	0.111	0.152	0.132	0.138	0.186	0.172

the conditions are similar to those for the mononuclear complex **3** except that a different molar ratio of 1 : 1 : 2 (Ln : HBpz$_3$: pba) was used, as described below.

To an aqueous solution of LnCl$_3$·6H$_2$O was added an aqueous solution of KHBpz$_3$ and an ethanolic solution of either K(*S*-pba) or K(*RS*-pba) with a molar ratio of 1 : 1 : 2 (Ln^{3+} : HBpz$_3$: pba) in a beaker. The mixture was stirred for 1 h. The white precipitate obtained was filtered off, dried under vacuum and recrystallized from dichloromethane–hexane solution. Single crystals suitable for X-ray analysis of [Ln$_2${μ-(*RS*-pba)}$_4$-(HBpz$_3$)$_2$] (Ln = Nd, Gd, Dy, Ho and Yb) and [Dy$_2${μ-(*S*-pba)}$_4$(HBpz$_3$)$_2$] were obtained by slow evaporation of the dichloromethane–hexane solution.

The formation of the dinuclear [Ln$_2${μ-(*S*- or *RS*-pba)}$_4$-(HBpz$_3$)$_2$] complexes was confirmed by elemental analysis and/or ESI-MS measurements on a Perkin Elmer API-III spectrometer. The *m/z* for the main peaks observed for the Ho–Ho and Nd–Nd complexes are 1409 for {[Ho$_2${μ-(*RS*-pba)}$_4$(HBpz$_3$)$_2$] + H$^+$} and 1367 for {[Nd$_2${μ-(*RS*-pba)}$_4$(HBpz$_3$)$_2$] + H$^+$}, respectively.

Elemental analysis: [Yb$_2${μ-(*RS*-pba)}$_4$(HBpz$_3$)$_2$]; Anal. Found: C, 48.9; H, 4.43; N 11.5%. Calcd for C$_{58}$H$_{64}$N$_{12}$O$_8$-B$_2$Yb$_2$: C, 48.7; H, 4.66; N, 11.7%. [Yb$_2${μ-(*S*-pba)}$_4$(HBpz$_3$)$_2$]; Anal. Found: C, 49.0; H, 4.49; N 11.7%. Calcd for C$_{58}$H$_{64}$-N$_{12}$O$_8$B$_2$Yb$_2$: C, 48.7; H, 4.66; N, 11.7%. [Ho$_2${μ-(*RS*-pba)}$_4$-(HBpz$_3$)$_2$]; Anal. Found: C, 49.4; H, 4.33; N 11.8%. Calcd for C$_{58}$H$_{64}$N$_{12}$O$_8$B$_2$Ho$_2$: C, 49.4; H, 4.72; N, 11.9%. [Ho$_2${μ-(*S*-pba)}$_4$-(HBpz$_3$)$_2$]; Anal. Found: C, 49.5; H, 4.56; N 11.7%. Calcd for C$_{58}$H$_{64}$N$_{12}$O$_8$B$_2$Ho$_2$: C, 49.4; H, 4.72; N, 11.9%. [Dy$_2$-{μ-(*S*-pba)}$_4$(HBpz$_3$)$_2$]; Anal. Found: C, 49.3; H, 4.48; N 11.9%. Calcd for C$_{58}$H$_{64}$N$_{12}$O$_8$B$_2$Dy$_2$: C, 49.6; H, 4.60; N, 11.9%. [Gd$_2${μ-(*RS*-pba)}$_4$(HBpz$_3$)$_2$]; Anal. Found: C, 50.6; H, 4.51; N 12.2%. Calcd for C$_{58}$H$_{64}$N$_{12}$O$_8$B$_2$Gd$_2$: C, 49.9; H, 4.77; N, 12.1%. [Nd$_2${μ-(*S*-pba)}$_4$(HBpz$_3$)$_2$]; Anal. Found: C, 50.4; H, 4.66; N 13.0%. Calcd for C$_{58}$H$_{64}$N$_{12}$O$_8$B$_2$Nd$_2$: C, 51.0; H, 4.72; N, 12.3%. [Nd$_2${μ-(*RS*-pba)}$_4$(HBpz$_3$)$_2$]; Anal. Found: C, 51.2; H, 4.87; N 10.46%. Calcd for C$_{58}$H$_{64}$N$_{12}$O$_8$B$_2$Nd$_2$: C, 51.0; H, 4.72; N, 12.3%. [Ho(pba)(HBpz$_3$)$_2$]; Anal. Found: C, 44.6; H, 4.52; N 21.3%. Calcd for C$_{28}$H$_{31}$N$_{12}$O$_2$B$_2$Ho: C, 44.6; H, 4.14; N, 22.3%. [Er(pba)(HBpz$_3$)$_2$]; Anal. Found: C, 42.0; H, 4.03; N 19.0%. Calcd for C$_{28}$H$_{31}$N$_{12}$O$_2$B$_2$Er·CH$_2$Cl$_2$·0.17C$_6$H$_{14}$: C, 42.1; H, 4.16; N, 19.6%.

Measurements

Absorption spectra were measured on a Perkin Elmer Lamda-19 spectrophotometer. CD data were collected on a Jasco J-720W spectropolarimeter. MCD spectra were recorded on a Jasco J-720W spectropolarimeter in a magnetic field of

1.5 T at room temperature. An attempt at CD measurement for [Ho(HBpz$_3$)$_2$(*S*-pba)] failed, probably because the CD intensity was too small to be observed, as inferred from the vicinal chirality.

X-Ray structure determination

[Ln$_2${μ-(*RS*-pba)}$_4$(HBpz$_3$)$_2$] (Ln = Nd, Gd, Dy, Ho and Yb) complexes. A colorless crystal of each [Ln$_2${μ-(*RS*-pba)}$_4$-(HBpz$_3$)$_2$] (Ln = Yb, Ho, Dy, Gd and Nd) complex was sealed in a glass capillary tube to prevent possible efflorescence. The X-ray intensities ($2\theta_{max}$ = 60°) were measured on a Rigaku AFC-5R four circle diffractometer at 23 °C. The structures were solved by the direct methods using the SHELXS86 program,[12] and refined on F^2 against all reflections by full-matrix least-squares techniques using SHELXL97.[13] All non-hydrogen atoms were treated anisotropically. All calculations were carried out using the TeXsan software package.[14]

[Dy$_2${μ-(*S*-pba)}$_4$(HBpz$_3$)$_2$] complex. A colorless crystal of [Dy$_2${μ-(*S*-pba)}$_4$(HBpz$_3$)$_2$] was mounted on a loop. All measurements were made on a Rigaku/MSC Mercury CCD diffractometer with graphite-monochromated Mo-Kα radiation at -73 °C. The structure solutions and refinements were performed as described for the racemic complexes. See Table 1 for all crystallographic data.
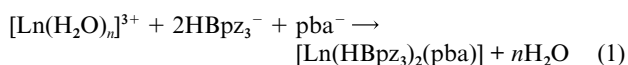
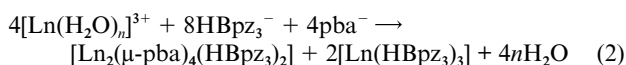CCDC reference numbers 210009–210014.

See http://www.rsc.org/suppdata/dt/b3/b304928k/ for crystallographic data in CIF or other electronic format.

Results and discussion

Synthesis of [Ln(*S*- or *RS*-pba)(HBpz$_3$)$_2$] and [Ln$_2${μ-(*S*- or *RS*-pba)}$_4$(HBpz$_3$)$_2$] complexes

The synthetic method for mononuclear [Ln(*S*- or *RS*-pba)$_4$-(HBpz$_3$)$_2$] (Method A) gave both mononuclear (Ho to Yb) and dinuclear [Ln$_2${μ-(*S*- or *RS*-pba)}$_4$(HBpz$_3$)$_2$] (Nd to Dy) complexes. We could not synthesize mononuclear complexes for Nd to Dy; only the dinuclear complexes were obtained by employing Method A (even by adding an excess amount of KHBpz$_3$), in contrast to the fact that a series of mononuclear acetate bridged Ln(III) complexes[15] have been obtained. This means that the formation reaction in Method A for the lighter Ln complexes proceeds according to eqn. (2), but not to eqn. (1).

$$[Ln(H_2O)_n]^{3+} + 2HBpz_3^- + pba^- \longrightarrow$$
$$[Ln(HBpz_3)_2(pba)] + nH_2O \quad (1)$$

$$4[Ln(H_2O)_n]^{3+} + 8HBpz_3^- + 4pba^- \longrightarrow$$
$$[Ln_2(\mu\text{-pba})_4(HBpz_3)_2] + 2[Ln(HBpz_3)_3] + 4nH_2O \quad (2)$$

However, with the stoichiometric molar ratio 1 : 1 : 2 (Ln^{3+} : KHBpz$_3$: pba) we could synthesize a series of dinuclear complexes (Nd to Yb) by an easier method under milder or ambient conditions compared to those with a molar ratio 1 : 1 : 2.2 (Ln^{3+} : KHBpz$_3$: CH_3COO^-) under inert conditions in boiling THF solution for $[Y_2\{\mu\text{-}(O_2CCH_3)\}_4(HBpz_3)_2]$.[6] The corresponding dinuclear acetate bridged Yb(III) complex $[Yb_2\{\mu\text{-}(O_2CCH_3)\}_4$-$(HBpz_3)_2]$ could not be obtained, and only the mononuclear acetate Yb complex $[Yb(O_2CCH_3)(HBpz_3)_2]$ was isolated by Method B. From these facts, the formation of mononuclear and dinuclear complexes is suggested to depend on the ionic radii of the lanthanide ions and/or to be controlled by the ratio of Ln : KHBpz$_3$: pba. In other words, this may result from two sources; the larger lanthanide ions prefer the formation of $[Ln(HBpz_3)_3]$ to that of the mononuclear complexes as seen for the synthesis of the Cr–Ln complexes[3] and the pba bridged dinuclear complexes may be more stable than the acetate bridged ones. In the course of the competitive reactions between eqn. (1) and (2) for the lighter Ln complexes, the reaction *via* eqn. (2) is more favorable than that *via* eqn. (1).

X-Ray structure analysis

Table 1 shows the crystallographic data for the Ln–Ln complexes. All the *meso*-(*RS*-pba) complexes crystallize in the $P\bar{1}$ space group with a triclinic crystal system. Fig. 1a and b show the ORTEP[16] views of the complex $[Ho_2\{\mu\text{-}(RS\text{-pba})\}_4$-$(HBpz_3)_2]$ where the phenyl and ethyl groups of the pba and the HBpz$_3$ groups are omitted respectively, for clarity. The holmium ion is seven-coordinate with four oxygen atoms from four μ-pba's and three nitrogen atoms from HBpz$_3$ as found for the Y, Sm, Eu, Gd, Tb complexes.[6,8,10] Two Ho ions are connected by four pba bridging groups. This μ-(*RS*-pba) complex is not a racemic mixture of the (μ-*R*-pba)$_4$ and (μ-*S*-pba)$_4$ complexes, but a *meso*-Ho$\{(\mu\text{-}R\text{-pba})_2(\mu\text{-}S\text{-pba})_2\}$Ho complex which is centrosymmetric with an inversion center at the midpoint between the Ln $\cdots$ Ln line, as found for the $[(H_2O)_4Ln(\mu\text{-DL-ala})_4$-Ln$(H_2O)_4]$ complexes.[8] The analogous Yb–Yb, Dy–Dy, Gd–Gd and Nd–Nd complexes are isostructural with the Ho–Ho one as shown in Fig. S1–S4, † respectively.

Of the two possible conformational isomers, with respect to the combination of the *R*- and *S*-pba in the bridging moiety, only the centrosymmetric *cis* isomer with a *R-R-S-S* assembly was stereospecifically formed for all of the complexes, but not the *trans* isomer with two mirror planes in a *R-S-R-S* assembly. This fact suggests that the *cis* positioning of two *R*-pba or *S*-pba is more favorable than the *trans* one probably owing to the steric contacts between the bulky substituents of the adjacent pba's. In the lanthanide(III) (Yb, Ho, Dy, Gd and Nd) complexes with HBpz$_3$, the coordination of the four carboxylates is classified as *Z,Z*-type bridging didentate.[17] Four CH–π interactions between the methyl protons of the ethyl groups of the pba and the phenyl group in the adjacent pba are found (*vide infra*). This steric control from the four CH–π interactions may stabilize seven-coordination of the Ln^{III} ion in the dinuclear system. The polyhedron around the Ln^{III} ions is a monocapped trigonal prism (*TPRS*-7) as described for the corresponding acetato bridged Y complex.[6]

Table 2 shows the selected bond lengths of the Ln–Ln complexes. The Ln–O and Ln–N distances increase from Yb to Nd in a regular manner, becoming longer with increasing ionic radius of the Ln^{III} ion as expected. The Yb–O and Nd–O distances range from 2.214(4)–2.298(5) Å and 2.362(5)–2.423(5) Å, respectively. The Yb–N and Nd–N distances range from 2.411(4)–2.446(4) Å and 2.565(5)–2.577(5) Å. However, neither O–Ln–O nor N–Ln–N angles show regular variation along the series. The non-bonding Yb $\cdots$ Yb (4.1022(7) Å), Ho $\cdots$ Ho
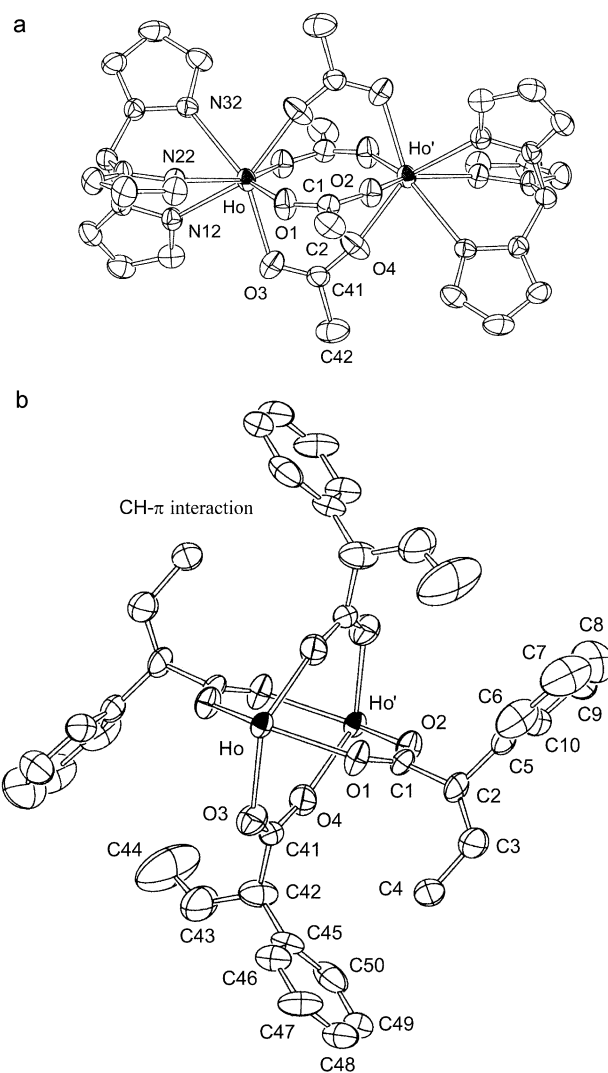

Fig. 1 ORTEP views of $[Ho_2\{\mu\text{-}(RS\text{-pba})\}_4(HBpz_3)_2]$ where the phenyl and ethyl groups (a) and the HBpz$_3$ group (b) are omitted for clarity.

(4.0817(11) Å), Dy $\cdots$ Dy (4.0651(15) Å), Gd $\cdots$ Gd (4.0290(9) Å) and Nd $\cdots$ Nd (4.0363(9) Å) distances in $[Ln_2$-$(\mu\text{-}RS\text{-pba})_4(HBpz_3)_2]$ are comparable to that (4.037 Å) in $[Y_2(\mu\text{-}CH_3CO_2)_4(HBpz_3)_2]$, but are longer than the Gd $\cdots$ Gd distances (3.9430(4) and 3.9148(4) Å, respectively) in $[Gd_2$-$(\mu\text{-OBz})_4(HBpz_3)_2]$ (OBz = benzoate) and $[Gd_2(\mu\text{-}p\text{-OBzCl})_4$-$(HBpz_3)_2]$,[10] and shorter than the Nd $\cdots$ Nd distances (4.412 and 4.439 Å) in dimeric $[Nd_2(\text{L- and DL-}\alpha\text{-Ala})_4(H_2O)_8](ClO_4)_6$.[8] The Ln $\cdots$ Ln distances increase from Nd to Yb almost regularly. It is noted that the larger the ionic radius of the central Ln ion, the shorter the Ln $\cdots$ Ln distance with the exception of the Nd complex.

For the chiral *S*-pba Ln–Ln complexes, it was hard to obtain crystals suitable for X-ray analysis. However, fortunately, we could crystallize chiral $[Dy_2\{\mu\text{-}(S\text{-pba})_4\}(HBpz_3)_2]$ suitable for single crystal X-ray analysis. Two crystallographically independent molecules in the unit cell of the chiral *S*-pba Dy–Dy complex are structurally somewhat different from each other as mentioned below (see also Table 2). One of them is shown in Fig. 2. Each Dy(III) ion is linked by four oxygen atoms from the bridging pba. In addition to the normal Dy–O bonding, two oxygens are bonded in a bifurcated three center (Dy–(μ-O) $\cdots$ Dy) mode which belongs to a bridging tridentate type as found for $Ln_2(\eta^1\!:\!\eta^1\!:\!\mu_2\text{-}CH_3CO_2)_2(\eta^2\!:\!\eta^1\!:\!\mu_2\text{-}CH_3CO_2)_2$ in the Ce(III) complex, $[Ce_2(\mu\text{-}CH_3CO_2)_6(phen)_2]$.[7] Thus, this complex was found to have each pseudo-eight-coordinated Dy(III) ion in contrast to the *meso*-$[Dy_2\{\mu\text{-}(RS\text{-pba})\}_4(HBpz_3)_2]$ complexes with centrosymmetric ill-defined

Table 2 Selected bond lengths (Å) and non-bonding distances (Å)

1		2		5		6				3		4	
Ln · · · Ln distance													
Yb · · · Yb′	4.1022(7)	Ho · · · Ho′	4.0817(11)	Dy · · · Dy′	4.0651(15)	Dy1 · · · Dy2	3.8578(9)	Dy11 · · · Dy12	3.9590(9)	Gd · · · Gd′	4.0290(9)	Nd · · · Nd′	4.0363(9)
Ln–O bond lengths													
Yb–O1	2.265(4)	Ho–O1	2.293(5)	Dy–O1	2.304(5)	Dy1–O2	2.378(10)	Dy11–O12	2.361(14)	Gd–O1	2.329(4)	Nd–O1	2.374(5)
						Dy2–O1	2.237(9)	Dy12–O11	2.268(10)				
Yb–O2′	2.236(4)	Ho–O2′	2.275(4)	Dy–O2′	2.290(5)	Dy1–O3	2.308(9)	Dy11–O13	2.291 (11)	Gd–O2′	2.328(3)	Nd–O2′	2.395(5)
						Dy2–O4	2.368(10)	Dy12–O14	2.308(12)				
Yb–O3	2.298(5)	Ho–O3	2.326(6)	Dy–O3	2.342(7)	Dy1–O5	2.311(10)	Dy11–O15	2.304(9)	Gd–O3	2.380(4)	Nd–O3	2.423(5)
						Dy2–O6	2.333(9)	Dy12–O16	2.262(9)				
Yb–O4′	2.214(4)	Ho–O4′	2.248(5)	Dy–O4′	2.263(6)	Dy1–O7	2.306(10)	Dy11–O17	2.287(9)	Gd–O4′	2.307(4)	Nd–O4′	2.362(5)
						Dy2–O8	2.255(10)	Dy12–O18	2.294(10)				
						Dy1–O1	2.593(9)	Dy11–O11	2.736(11)				
				Dy2–O3	2.731(10)								
Non-bonding Ln · · · O distances													
Yb · · · O2	3.748(5)	Ho · · · O2	3.753(6)	Dy · · · O2	3.771(7)			Dy12 · · · O13	3.09(1)	Gd · · · O2	3.782(4)	Nd · · · O4	3.763(6)
Yb · · · O4	3.416(6)	Ho · · · O4	3.272(7)	Dy · · · O4	3.173(9)					Gd · · · O4	2.992(5)	Nd · · · O2	2.945(6)
Ln–N bond lengths													
Yb–N12	2.446(4)	Ho–N12	2.488(5)	Dy–N12	2.492(6)	Dy1–N12	2.469(13)	Dy11–N112	2.470(14)	Gd–N12	2.522(4)	Nd–N12	2.577(5)
						Dy2–N17	2.462(11)	Dy12–N117	2.459(11)				
Yb–N22	2.411(4)	Ho–N22	2.450(5)	Dy–N22	2.468(6)	Dy1–N22	2.456(12)	Dy11–N122	2.497(12)	Gd–N22	2.508(4)	Nd–N22	2.565(5)
						Dy2–N27	2.488(12)	Dy12–N127	2.493(12)				
Yb–N32	2.436(4)	Ho–N32	2.478(5)	Dy1–N32	2.490(6)	Dy2–N35	2.500(12)	Dy11–N132	2.511(10)	Gd–N32	2.510(4)	Nd–N32	2.568(5)
						Dy2–N37	2.496(13)	Dy12–N137	2.498(14)				

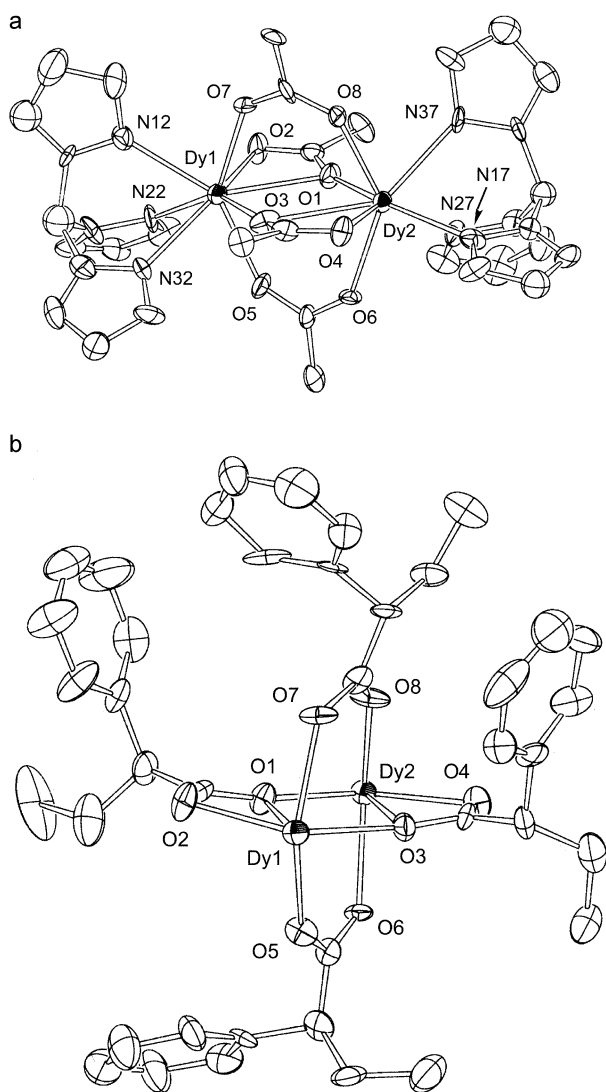**Fig. 2** ORTEP views of [Dy$_2${μ-(*S*-pba)}$_4$(HBpz$_3$)$_2$] where the phenyl and ethyl groups (a) and the HBpz$_3$ group (b) are omitted for clarity.

Fig. 3 Molecular models of only the bridging moiety (a) [Dy$_2${μ-(*RS*-pba)}$_4$(HBpz$_3$)$_2$] complex with weak CH–π interactions between the methyl proton in the ethyl group of the pba and the phenyl ring of the adjacent pba for the *rac*-pba complex. (b) [Dy$_2${μ-(*S*-pba)}$_4$(HBpz$_3$)$_2$] has no such interactions.

seven-coordination. The average non-bonding Dy · · · Dy distance is 3.9084 Å, which is shorter than that (4.0651(15) Å) in the *meso*-Dy–Dy complex.

Moreover, the Dy · · · (μ-O) non-bonding distance (for example, Dy12 · · · O13 is 3.09(1) Å) in the *chiral*-Dy–Dy complex is much shorter than the shortest non-bonding Dy · · · O2 and Dy · · · O4 distance 3.771(7) Å and 3.173(9) Å in the *meso*-Dy–Dy complex. Shortening in the Dy · · · Dy distance is associated with shortening in the Dy · · · O one. One of the two oxygen atoms involved in the non-bonding interaction in the Dy–(μ-O) · · · Dy of the chiral complex occupies the capping position on the lateral face of four oxygen atoms around the Dy, forming a bicapped trigonal prism (*TPRS*-8). This indicates the seven- and pseudo-eight-coordinate character in the *meso*- and *chiral*-Dy–Dy dinuclear complexes, respectively, though another chiral complex in the unit cell has seven- and pseudo-eight-coordinated Dy moieties (Table 2 and Fig. S5†). These differences in interatomic distance may result from differences in the packing among the bridging pba's between the *meso*- and *chiral*-(*S*-pba) Dy–Dy complexes. That is, there exists four weak CH–π interactions between the methyl proton in the ethyl group of one pba and the phenyl ring of the adjacent pba for the *meso*-pba complexes (*vide supra*; Fig. 3), since the carbon(methyl)–carbon(phenyl) distance between them is found to be about 3.7 Å. However, there is no CH–π interaction in the *chiral*-(*S*-pba) Dy–Dy complex. Such a difference in the intramolecular interactions may lead to the difference in the
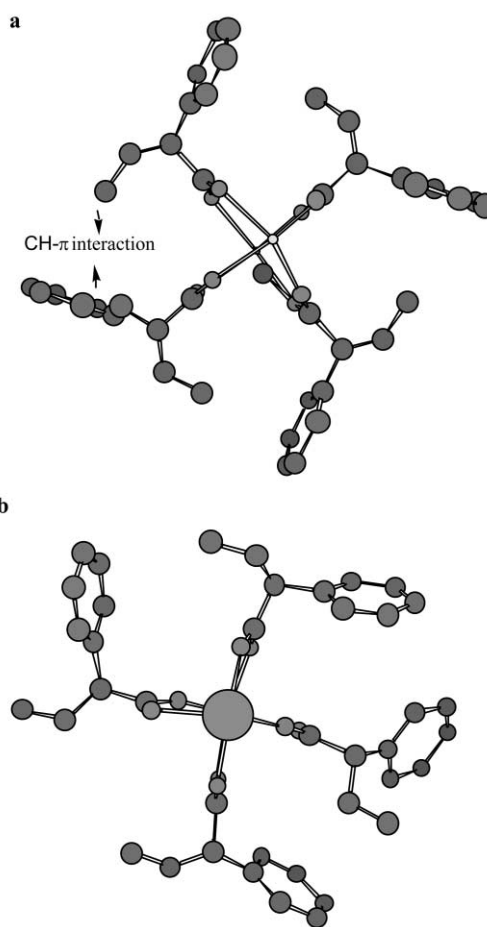
non-bonding Dy · · · Dy as well as the Dy · · · O distances. The intramolecular CH–π interaction could prevent two Dy moieties from approaching each other and would maintain the high symmetry of the bridging moiety in the *meso*-(*RS*-pba) Ln–Ln complexes. Shortening of the Ln · · · O distances with increasing Ln^{III} ion size from Yb to Nd may be parallel to a decrease in the non-bonding Ln · · · Ln distance, or may reflect the tendency of increasing coordination number with increasing Ln ion size as shown in Table 2. Taking into consideration these facts, there might be some attractive interatomic non-bonding interaction between the Ln and O as also found for [(hfac)$_3$Ln(bpypz)Cr(acac)$_3$] (hfac = hexafluoroacetylacetone, bpypz = 3,5-bis(2-pyridyl)pyrazolate) complexes.[18]

For the chiral complexes, there are two kinds of possible configurational chirality in the tetrakis-carboxylate bridged dinuclear complexes. One is a twisted configuration around the metal–metal vector in the bridging moiety. However, the X-ray structure of the present chiral Dy–Dy complex demonstrates the existence of an almost eclipsed configuration with a mirror plane, resulting in an achiral bridging moiety as found in corresponding types of transition metal complexes such as [Rh$_2$(O$_2$CR)$_4$L$_2$] where R = CPh(OH)H and CPh(OMe)H.[11] The other is a new type arising from the relative skew disposition of two B · · · Dy vectors. That is, the B · · · Dy · · · Dy · · · B arrangement in the *chiral*-(*S*-pba) Dy–Dy complex is bent with an average torsion angle of 50°, in contrast to the linear arrangement with a torsion angle of 180° in the *meso*-(*RS*-pba) Dy–Dy complex. According to the definition that one B · · · Dy line is overlapped with the other B · · · Dy line by a clockwise (*C*) or anticlockwise (*A*) rotation around the Dy · · · Dy line, the configurational chirality in the *chiral*-

Complex	Transition (λ/nm) $g = \Delta\varepsilon/\varepsilon$	Ln(μ-S-pba)$_4$Ln $g = \Delta\varepsilon/\varepsilon$		Cr(ox)Ln g(Ln–Ln)/g(Cr–Ln)
Yb	$^2F_{7/s} \longrightarrow {}^2F_{5/2}$ (975)	2.8×10^{-4}	6.0×10^{-2}	4.7×10^{-3}
Ho	$^5I_8 \longrightarrow {}^5I_5$ (890)	6.0×10^{-5}	1.2×10^{-4}	5.0×10^{-1}
Dy	$^6H_{15/2} \longrightarrow {}^6F_{7/2}$ (900)	2.5×10^{-4}	2.0×10^{-3}	1.3×10^{-1}
Nd	$^4I_{9/2} \longrightarrow {}^4F_{5/2}$ (800)	2.6×10^{-4}	6.6×10^{-4}	3.7×10^{-1}

[Yb(S-pba)(HBpz$_3$)$_2$] gives g(Yb) = 2.4×10^{-3} and therefore g(Yb)/g(Cr–Yb) = 3.8×10^{-2}.

(S-pba) Dy–Dy complex is described as C in Fig. 4. This new configurational chirality will be discussed in connection with the CD in the 4f–4f transitions below.
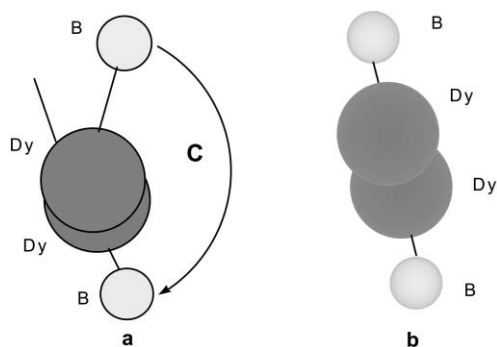

Fig. 4 Views of the molecular models along the Dy–Dy line showing the configurational chirality (C) and achirality, respectively. (a) [Dy$_2$-{μ-(S-pba)}$_4$(HBpz$_3$)$_2$] complex with a bent B $\cdots$ Dy $\cdots$ Dy $\cdots$ B arrangement (*ca.* 50°). (b) [Dy$_2${μ-(RS-pba)}$_4$(HBpz$_3$)$_2$] complex with a linear B $\cdots$ Dy $\cdots$ Dy $\cdots$ B arrangement (180°).

NIR chiroptical study

The NIR absorption, MCD and CD spectra of [Ln$_2${μ-(S- or RS-pba)}$_4$(HBpz$_3$)$_2$] (Ln = Yb, Ho, Dy and Nd) complexes were measured in CH$_2$Cl$_2$ solution. For [Yb$_2${μ-(RS-pba)}$_4$(HBpz$_3$)$_2$], the strongest peak of the NIR absorption spectra in the $^2F_{7/2} \longrightarrow {}^2F_{5/2}$ transitions are observed around 975 nm similar to those of [(acac)$_2$Cr(μ-ox)Yb(HBpz$_3$)$_2$] and [Yb(RS-pba)(HBpz$_3$)$_2$] as in Fig. 5. In the corresponding region, MCD spectra show a similar behavior to each other; a strong couplet of (−) and (+) at the longer wavelength is observed. The other shorter wavelength absorption and MCD peaks are different from each other as in Fig. 5. The complex [Yb$_2${μ-(S-pba)}$_4$(HBpz$_3$)$_2$] shows three CD bands corresponding to the $^2F_{7/2} \longrightarrow {}^2F_{5/2}$ transitions in the 900–1000 nm region. The CD pattern and sign sequences are different from those of the (Λ–Δ)-Cr(μ-ox)Yb[3] and Λ-[Yb(DOTMA)]$^-$ (DOTMA = $1R,4R,7R,10R$-α,α',α'', α'''-tetramethyl-1,4,7,10-tetraazacyclododecane-1,4,7,10-tetraacetate) complexes.[19] This may be due to the difference in coordination number or crystal field among the Yb(O)$_4$(N)$_3$, Yb(O)$_2$(N)$_6$ and Yb(O)$_4$(N)$_4$ chromophores. The dissymmetry factor ($g = \Delta\varepsilon_{ext}/\varepsilon_{max}$) at 975 nm for the Yb–Yb complex is *ca.* 2.8×10^{-4} which is small compared to that of (Λ–Δ)-[(acac)$_2$-Cr(ox)Yb(HBpz$_3$)$_2$] as well as that of the mononuclear [Yb-(HBpz$_3$)$_2$(S-pba)].[3a] This observed difference in g values between the dinuclear and mononuclear S-pba Yb complexes is explained in relation to the configurational chirality as discussed below.

For the other chiral Ln–Ln complexes, the NIR CD components (Fig S6–S8 †) are assigned to the following 4f–4f transitions in comparison with the NIR absorption spectra of the *meso*-Ln–Ln complexes; $^5I_8 \longrightarrow {}^5I_5$ at 890 nm for the Ho–Ho, $^6H_{15/2} \longrightarrow {}^6F_{7/2}$, $^6H_{15/2} \longrightarrow {}^6F_{5/2}$ and $^6H_{15/2} \longrightarrow {}^6F_{3/2}$ at 700–950 nm for the Dy–Dy, and $^4I_{9/2} \longrightarrow {}^2H_{9/2}$, $^4I_{9/2} \longrightarrow {}^4F_{5/2}$, $^4I_{9/2} \longrightarrow {}^4F_{3/2}$ at 850–950 nm for the Nd–Nd complex. The assignments are confirmed by the MCD measurements as in Fig. S6–S8. †
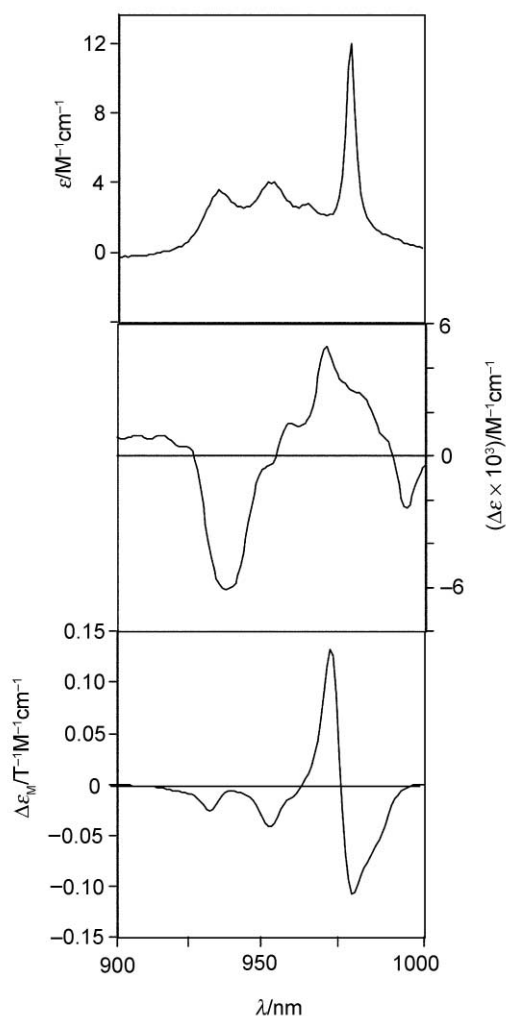

Fig. 5 NIR absorption (top) and CD (middle) spectra of [Yb$_2${μ-(S-pba)}$_4$(HBpz$_3$)$_2$] and MCD (bottom) spectra of [Yb$_2${μ-(RS-pba)}$_4$(HBpz$_3$)$_2$] in CH$_2$Cl$_2$ at room temperature.

These CD intensities may arise from vicinal chirality due to the asymmetric carbon in S-pba as well as the configurational one due to the skew B $\cdots$ Ln dispositions as found from the X-ray structure of the chiral Dy(S-pba)$_4$Dy complex (*vide supra*). In order to examine the CD origins, it is appropriate to compare the dissymmetry factors $g = \Delta\varepsilon_{ext}/\varepsilon_{max}$ for CD components in the Ln–Ln complexes as shown in Table 3. This is because these CD components are due to the same 4f–4f transitions common to those for the Cr–Ln complexes which are proposed to be a common criterion for the relation[3b] between the CD signs and the absolute configuration around the Ln(HBpz$_3$)$_2$(ox) moiety. Comparison between the ratios g(Ln–Ln)/g(Cr–Ln) and g(Yb)/g(Cr–Yb)[3] allow us to predict whether the 4f–4f CD for the Ln–Ln complexes arise from either configurational or vicinal chirality, irrespective of any type of 4f–4f transitions which are magnetic-dipole allowed for the Yb^{III} complexes or forbidden for the Ho^{III}, Dy^{III} and Nd^{III} complexes according to the selection rules.[20] The g(Ln–Ln) values for the Ho, Dy, and Nd complexes are not much different from the

corresponding g(Cr–Ln) ones as shown in Table 3. Moreover, the g(Ln–Ln)/g(Cr–Ln) ratios are similar to one another and much larger than the g(Yb)/g(Cr–Yb) ones. These facts suggest additional configurational contribution other than the vicinal one due to S-pba to CD intensity. In other words, configurational chirality due to the B $\cdots$ Ln skew dispositions produces about a ten times larger g(Ln–Ln)/g(Cr–Ln) ratio for the Ho, Dy, and Nd complexes than g(Yb)/g(Cr–Yb) (Table 3). The g(Yb–Yb)/g(Cr–Yb) for the Yb–Yb complex is about one hundredth of those for the other Ln–Ln complexes. This is probably due mostly to the vicinal chirality from the S-pba moiety in the Yb–Yb complex. As inferred from the fact that a series of the *meso*-Ln–Ln complexes shows Ln^{III} ion size dependent changes of the non-bonding Ln $\cdots$ O and Ln $\cdots$ Ln distances (*vide supra*), the S-pba Yb–Yb complex with the smallest Ln^{III} ion radius among them is assumed to be seven-coordinate with longer Ln $\cdots$ O and Ln $\cdots$ Ln distances like the *meso* Ln–Ln complexes rather than a pseudo-eight one, in line with a decreasing tendency of the coordination number from the other large Ln^{III} to the small Yb^{III}. Thus, the small g(Yb–Yb)/g(Cr–Yb) is suggested to have an almost achiral configuration due to the B $\cdots$ Ln $\cdots$ Ln $\cdots$ B linear arrangement as found for the *meso*-Ln–Ln complexes. This may reflect the weak CD behaviors for the Yb(S-pba)$_4$Yb complex in solution. Further investigation is needed to clarify the structural differences among the Ln(S-pba)$_4$Ln complexes.

Conclusions

Synthesis of two series of mononuclear [Ln(S- or RS-pba)-(HBpz$_3$)$_2$] and dinuclear [Ln$_2$\{μ-(S- or RS-pba)\}$_4$(HBpz$_3$)$_2$] complexes are described, the formation of which depends on the lanthanide ionic radius and/or steric control of the pba. The X-ray structural analysis of some of the complexes demonstrate stereospecific formation of the R-R-S-S assembly in the bridging moiety of the *meso*-(μ-R,S-pba)$_4$ complexes with seven-coordination and high symmetry. This ordered structure may result from weak CH–π interactions between one pba and the adjacent pba. The Dy(μ-S-pba)$_4$Dy complex is found to have configurational chirality due to the B $\cdots$ Ln skew bent arrangement from the X-ray analysis. Such a chiral configuration is corroborated by examining the dissymmetry factors of the chiral S-pba Ho, Dy, and Nd complexes. The smaller g value of the heavier Yb–Yb complex compared to that of the Cr–Yb complex may be due to vicinal chirality in the S-pba moiety. This fact reconfirms the configurational chiral assembly in the Cr(μ-ox)Ln complexes. Further comparative studies in relation to the structural, magnetic and spectroscopic properties between the *meso*-(RS-pba) and *chiral*-(S-pba) complexes are in progress in this laboratory.

References

1 (*a*) J.-C. G. Bünzil and C. Piguet, *Chem. Rev.*, 2002, **102**, 1897; (*b*) D. Parker, R. S. Dickins, H. Puschmann, C. Crossland and J. A. K. Howard, *Chem. Rev.*, 2002, **102**, 1977 and references therein.
2 (*a*) T. Sanada, T. Suzuki and S. Kaizaki, *J. Chem. Soc., Dalton, Trans.*, 1998, 959; (*b*) T. Sanada, T. Suzuki, T. Yoshida and S. Kaizaki, *Inorg. Chem.*, 1998, **37**, 4712.
3 (*a*) M. A. Subhan, T. Suzuki and S. Kaizaki, *J. Chem. Soc., Dalton, Trans.*, 2001, 492; (*b*) M. A. Subhan, T. Suzuki and S. Kaizaki, *J. Chem. Soc., Dalton. Trans.*, 2002, 1416.
4 M. A. Subhan, T. Sanada, T. Suzuki and S. Kaizaki, *Inorg. Chim. Acta*, 2003, **353C**, 263.
5 (*a*) M. A. Subhan, H. Nakata, T. Suzuki, J.-H. Choi and S. Kaizaki, *J. Lumin.*, 2003, **101**, 307; (*b*) M. A. Subhan, T. Suzuki and S. Kaizaki, *Mol. Cryst. Liq. Cryst.*, 379, **2002**, 395.
6 D. L. Reger, J. A. Lindeman and L. Lebioda, *Inorg. Chem.*, 1988, **27**, 3923.
7 A. Panagiotopoulous, S. P. Perlepes, E. Bakalbassis, I. Masson-Ramde, O. Khan, A. Terzis and C. P. Raptopoulou, *Inorg. Chem.*, 1995, **34**, 4918.
8 T. Glowiak, J. Legendziewicz, E. Huskowaska and P. Gawryszewska, *Polyhedron*, 1996, **15**, 2939 and references therein.
9 D. L. Reger, S. J. Knox, J. A. Lindeman and L. Lebioda, *Inorg. Chem.*, 1990, **29**, 416.
10 U. P. Singh, S. Tyagi, C. L. Sharma, H. Görner and T. Weyhermüller, *J. Chem. Soc., Dalton Trans.*, 2002, 4464.
11 (*a*) P. A. Agaskar, F. A. Cotton, L. R. Falvello and S. Hann, *J. Am. Chem. Soc.*, 1986, **108**, 1214; (*b*) F. A. Cotton, R. A. Walton, *Multiple bonds between metal atoms*, Clarendon Press, Oxford, 2nd edn., 1993 and references therein.
12 G. M. Sheldrick, *Acta Crystallogr., Sect. A*, 1990, **46**, 467.
13 G. M. Sheldrick, SHELXL97, University of Gottingen, Germany, 1997.
14 TeXsan, Single Crystal Structure Analysis Software, ver. 1.9, Molecular Structure Corporation, The Woodlands, TX and Rigaku Co. Ltd., Akishima, Tokyo, 1998.
15 M. A. J. Moss and C. J. Jones, *J. Chem. Soc., Dalton Trans.*, 1990, 581.
16 C. K. Johnson, ORTEP II, Report ORNL-5138, Oak Ridge National Laboratory, Oak Ridge, TN, 1976.
17 A. Ouchi, Y. Suzuki, Y. Ohki and Y. Koizumi, *Coord. Chem. Rev.*, 1988, **92**, 29.
18 R. Kawahata, T. Tsukuda, T. Yagi, M. A. Subhan, A. Fuyuhiro and S. Kaizaki, *Chem. Lett.*, 2003, in press.
19 L. Di Bari, G. Pintacuda and P. Salvadori, *J. Am. Chem. Soc.*, 2000, **122**, 5557; L. Di Bari, G. Pintacuda, P. Salvadori, R. S. Dickens and D. Parker, *J. Am. Chem. Soc.*, 2000, **122**, 9257.
20 F. S. Richardson, *Inorg. Chem.*, 1980, **19**, 2806.